doi.org/10.36721/PJPS.2026.39.1.REG.14912.1

Bruceine A alleviates lung injury in sepsis-associated acute respiratory distress syndrome by modulating macrophage polarization and NF-κB pathway activity

Jianlei Lv, Songbai Wu, Min Liu and Kang Huang*
Department of Critical Care Medicine, The First Hospital of Changsha, Changsha, Hunan, China

Abstract: **Background**: Sepsis-associated acute respiratory distress syndrome (ARDS) is a severe inflammatory lung disorder with high mortality. Bruceine A (BA), a quassinoid from *Brucea javanica*, exhibits anti-inflammatory and immunomodulatory activities, but its role in ARDS is unclear. **Objectives**: This study evaluated the protective effects of BA in lipopolysaccharide (LPS)-induced ARDS and explored its underlying mechanisms. **Methods**: Thirty-six C57BL/6 mice were randomized into four groups: control, LPS, LPS+BA and LPS+dexamethasone (Dex). Lung injury was assessed by histopathology, wet/dry weight ratio and TUNEL assay. Cytokine levels (TNF-α, IL-6, IL-1β, IL-10) were measured by ELISA. Macrophage polarization markers (iNOS, COX-2, Arg-1, YM1, CD206) and NF-κB pathway proteins were evaluated using immunohistochemistry and Western blotting. **Results**: BA significantly alleviated LPS-induced lung injury, reducing edema, tissue damage and alveolar apoptosis. It suppressed proinflammatory cytokines while enhancing IL-10. BA shifted macrophage polarization from proinflammatory M1 toward anti-inflammatory M2 phenotypes. Furthermore, BA inhibited NF-κB activation, evidenced by reduced phosphorylated p65 and restored IκBα levels. These effects were comparable to Dex. **Conclusion**: BA protects against LPS-induced ARDS in mice by modulating cytokine release, promoting M2 macrophage polarization and suppressing NF-κB activation. These findings suggest BA as a promising natural immunomodulatory agent for inflammatory lung diseases.

Keywords: Acute respiratory distress syndrome; Bruceine A; Macrophage polarization; NF-κB

Submitted on 26-07-2025 – Revised on 30-09-2025 – Accepted on 09-10-2025

INTRODUCTION

Sepsis, caused by infection, manifests as a systemic immune-inflammatory reaction and may progress to multi-organ failure, among which acute respiratory distress syndrome (ARDS) constitutes one of the most severe sequelae, with a mortality rate of 30-50% (Sygitowicz and Sitkiewicz, 2021, Gorman, *et al*., 2022, Arina and Singer, 2021). ARDS is characterized by alveolar-endothelial barrier disruption, pulmonary edema and inflammatory infiltration, leading to impaired gas exchange and hypoxemia. (Feng, *et al*., 2021, Huang, *et al*., 2024). Current treatment strategies for ARDS mainly rely on lung-protective ventilation, fluid management and glucocorticoid therapy (Banavasi, *et al*., 2021, Chang, *et al*., 2022). However, these approaches fail to adequately suppress the inflammatory response and long-term glucocorticoid use may cause immunosuppression and metabolic disturbances (Chastain, *et al*., 2024). Therefore, developing therapeutic strategies that can precisely regulate inflammation and promote lung tissue repair is of great clinical importance for sepsis-associated ARDS.

Macrophages serve as critical modulators of pulmonary inflammation and act as major determinants in the initiation and evolution of sepsis-associated ARDS (Liu, *et al*., 2025). Depending on their functional status, macrophages are polarized toward M1 or M2 subtypes. The M1 subset contributes to the initial stages of antimicrobial defense by releasing proinflammatory cytokines, including interleukin-1β (IL-1β), interleukin-6 (IL-6) and tumor necrosis factor-α (TNF-α), as well as producing reactive oxygen species and nitric oxide (Pérez and Rius-Pérez, 2022). However, excessive activation of M1 macrophages can result in uncontrolled inflammation, exacerbate lung tissue damage and accelerate ARDS progression (Liu, *et al*., 2022a). In contrast, M2 macrophages enhance tissue repair and suppress excessive inflammation by secreting anti-inflammatory mediators such as IL-10, mannose receptor (Mrc1/CD206) and arginase-1 (Arg-1) (Wang and Wang, 2023, Arora, *et al*., 2018). However, during the development of sepsis-associated ARDS, an imbalance in M1/M2 polarization leads to sustained inflammatory activation, thereby aggravating lung damage. Evidence suggests that the cytokines IL-4, together with IL-13, can induce M2 macrophage polarization and alleviate pulmonary damage, but their therapeutic application is limited by the complexity of the immune microenvironment (Cheng, *et al*., 2021). Additionally, NF-κB pathway activity has been evidenced to suppress the proinflammatory effects of M1 macrophages while promoting M2 macrophage function, thereby effectively alleviating lung injury (Wang and He, 2022). For instance, in sepsis-triggered acute lung injury (ALI) mouse models, certain natural compounds facilitate M2 polarization and suppress M1 polarization by targeting NF-κB, significantly reducing lung damage and mortality (Luan, *et al*., 2021). However, specific drugs targeting macrophage polarization remain scarce in clinical practice, highlighting the urgent

**Corresponding author:* e-mail: hhhakkk@163.com

need to explore novel immunoregulatory agents to treat sepsis-associated ARDS. Natural compounds have attracted attention for their safety, multi-target effects and immunomodulatory properties. Compared to synthetic drugs, plant-derived compounds typically exhibit lower toxicity, greater biocompatibility and the ability to modulate multiple inflammatory pathways simultaneously. These advantages make natural products particularly suitable for chronic or systemic inflammatory diseases, such as ARDS (Gouda, *et al*., 2023). Bruceine A (BA) is a natural quassinoid molecule primarily derived from *Brucea javanica*, a medicinal plant extensively applied in traditional Chinese medicine. Fig. 1 illustrates the chemical structure of BA. Recent research has revealed its anti-inflammatory, antitumor, as well as immunomodulatory properties (Zhang, *et al*., 2023). It has been shown that BA exerts anti-inflammatory effects by inhibiting the NF-κB and MAPK signaling pathways, thereby significantly reducing the expression of proinflammatory cytokines such as TNF-α and IL-6 (He, *et al*., 2021). Additionally, BA can regulate cell growth and differentiation via the PI3K/Akt pathway, suggesting a potential role in immune modulation (Zhang, *et al*., 2023). However, whether BA can treat sepsis-associated ARDS by modulating M1/M2 macrophage polarization remains unclear.

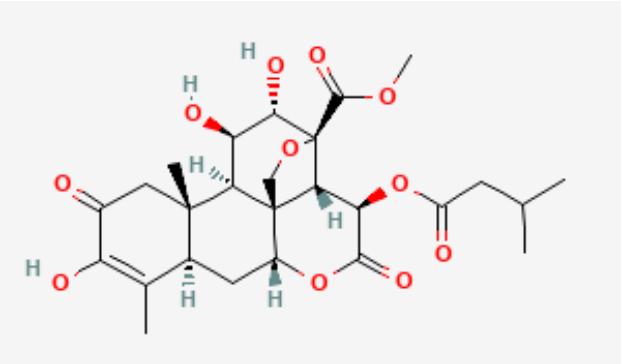

Fig. 1: Chemical structure of Bruceine A.

Accordingly, we utilized an ARDS mouse model triggered by lipopolysaccharide (LPS) to evaluate the protective role and mechanistic basis of BA in sepsis-associated ARDS. Lung tissue injury, inflammatory cytokines and markers of M1/M2 macrophage polarization were comprehensively analyzed. The study is expected to contribute to the development of immunoregulatory therapies for ARDS and explore new applications of natural products in inflammation-related diseases.

MATERIALS AND METHODS

Animal modeling and drug administration

This study used C57BL/6 male mice (aged 8–10 weeks, 20–25 g; Charles River Laboratories, Beijing, China). Mice were acclimated for one week at the animal center before experiments to ensure a stable health status. Sepsis-associated ARDS was induced via a one-time intraperitoneal (i.p.) administration of LPS (10 mg/kg, Cat#L2630, serotype O111:B4, Sigma-Aldrich) on day 0 of the experiment (Kim, *et al*., 2022, Ge, *et al*., 2024). To investigate the protective efficacy of BA, mice were allocated to four groups at random (n=9/group) with a computer-based randomization table: (a) Control group: i.p. phosphate-buffered saline (PBS) injection (equal volume, without LPS); (b) Sepsis group: LPS-induced ARDS without drug intervention; (c) LPS+BA group: LPS-induced ARDS with daily i.p. injection of BA (20 mg/kg, ≥96%, Cat#B860733, Macklin) for 3 consecutive days; (d) LPS +Dex group: LPS-induced ARDS with daily i.p. administration of dexamethasone (Dex, 5 mg/kg, Cat#D4902, Sigma-Aldrich) for 3 consecutive days, serving as a positive control.

The BA dose was determined based on structurally related compounds reported in previous research (Nie, *et al*., 2021), as well as on preliminary dose-finding experiments conducted in our laboratory. BA and Dex were freshly prepared in PBS before each injection. All injections were administered at 10 mL/kg body weight.

Throughout the 3-day treatment and observation period, all mice were monitored daily for behavioral changes, activity, grooming behavior and body weight. No mortality occurred in any group, resulting in a 100% survival rate. At study termination, mice were sacrificed and lung tissue, along with serum samples, were harvested for subsequent evaluation.

Hematoxylin-eosin (H&E) staining

Lung samples were immersed in 4% paraformaldehyde (Cat#P6148, Sigma-Aldrich) (24 h), paraffin-embedded and cut into slices of 5 μm. After deparaffinization and hydration, slices were H&E stained (Cat#G1120) and observed using an Olympus BX53 light microscope (Japan) for tissue pathology. Lung injury was scored by a blinded pathologist, evaluating alveolar exudation, capillary congestion, neutrophil infiltration, hemorrhagic changes, cellular remnants and cellular proliferation. The degree of injury was scored using a modified Smith grading scale (0-4), based on parameters including pulmonary edema, lung collapse, necrosis, alveolar/interstitial inflammatory infiltration, bleeding and hyaline membrane deposition, where 0 = no injury, 1 = 25% involvement, 2 = 50%, 3 = 75% and 4 = diffuse damage (Zhang, *et al*., 2021).

Immunohistochemistry assay

After deparaffinization and hydration, tissue slices were treated with 3% H_2O_2 at room temperature (10 min) to inactivate endogenous peroxidase, then a 10-min microwave-mediated antigen retrieval in citrate buffer (pH 6.0) was applied. Samples were subsequently pretreated with goat serum (30 min) and kept overnight at 4°C with primary antibodies specific to iNOS (ab15323) and CD206 (ab64693). The next day, after PBS washes, the slides were exposed to an HRP-labeled secondary antibody (1:500,

ab6721, Abcam) at 37°C for 30 minutes, followed by DAB staining, hematoxylin counterstaining, graded ethanol dehydration, xylene clearing and mounting with neutral resin. The expression and distribution of iNOS and CD206 in lung tissues were observed under a light microscope (Olympus BX53, Japan) (Zeng, *et al*., 2023). Image analysis was performed using ImageJ software (Version 1.53, National Institutes of Health, USA). Five randomly chosen high-power fields (400×) were analyzed and the ratio of positive cell area was quantified. All evaluations were performed under double-blind conditions by two independent pathologists.

Determination of lung wet weight/dry weight (W/D) ratio

Following euthanasia, lungs were excised promptly, with the trachea and surrounding connective tissues removed. Residual surface fluid was blotted dry with filter paper. Lung wet weight was measured using a balance and the data were recorded. Lungs were placed in an oven (60°C, 48 h) to constant weight and the dry mass was noted. The W/D ratio was computed to assess changes in lung water content (Wang, *et al*., 2024b).

TUNEL staining

After the cell treatment, 4% paraformaldehyde was used for fixation (30 min). Following PBS rinsing, the cells were permeabilized in 0.3% Triton X-100 (5 min, room temperature). Apoptosis was detected with the TUNEL assay kit (Cat#C1088, Beyotime, China). TUNEL reaction reagent was applied to each well and the cells were maintained at 37°C (60 min) in darkness. Afterward, they underwent three PBS washes (5 min per wash) to clear nonspecific binding. Thereafter, cells were stained with DAPI (10 min) and visualized by fluorescence microscopy. The apoptotic rate was quantified by measuring the ratio of TUNEL-positive cells to DAPI-stained cells via ImageJ (Version 1.53, National Institutes of Health, USA) (Ke, *et al*., 2021).

ELISA assay

After euthanizing the mice, blood samples were obtained by cardiac puncture. It was allowed to clot, followed by centrifugation (3000 rpm, 10 min, 4°C). The supernatant serum was collected and frozen at -80°C for future use. Bronchoalveolar lavage fluid (BALF) was obtained via bronchial intubation, with 1.5 mL of PBS used to lavage the lungs three times. The collected fluid was then centrifuged at 3000 rpm for 10 minutes at 4°C and the supernatant was stored at -80°C. The samples were incubated and color-reacted according to the instructions of the ELISA kits for TNF-α (Cat#PT512), IL-6 (Cat#PI326), IL-1β (Cat#PI301), as well as IL-10 (Cat#PI522) (Beyotime, China). The absorbance of each well was read at 450 nm with a microplate reader (Thermo Fisher Scientific, USA). The concentration of each inflammatory mediator in the serum and BALF (pg/mL) was calculated from the standard curve (Kang, *et al*., 2023). Each sample was analyzed in technical triplicate and data were obtained from three independent biological replicates.

Western blot

After euthanizing the mice, lung tissue was collected and placed in RIPA buffer (Cat#P0013C, Beyotime, China) with PMSF and phosphatase inhibitors (1% each). The tissue was homogenized on ice (30 min), then centrifuged (12,000 rpm, 15 min, 4°C). Supernatants were retained and protein content analyzed with BCA assay (Beyotime, P0012). After separation by SDS-PAGE, proteins were electroblotted onto PVDF membranes (Cat#IPVH00010, Millipore, USA) by wet transfer and blocked in 5% nonfat milk for 1 hour and treated with primary antibodies at 4°C overnight. Following PBS rinsing, HRP-linked secondary antibody (1:5000) was incubated with membranes at room temperature (1 h). Protein signals were detected by ECL and intensities quantified via ImageJ software (Version 1.53, National Institutes of Health, USA), normalized to β-actin (1:1000, ab8227, Abcam) (Ke, *et al*., 2021). The antibodies employed included: anti-iNOS (ab15323, Abcam), anti-COX2 (ab179800, Abcam), anti-Arginase 1 (Arg-1) (ab133543, Abcam), anti-Ym1 (#89984, CST), anti-p-NF-κB p65 (ab16502, Abcam) and anti-IκBα (ab32518, Abcam) (all 1:1000).

Statistical analysis

IBM SPSS Statistics 23.0 was utilized for statistical analyses. The Shapiro-Wilk test assessed data normality. When data met normality, they were reported as the mean ± standard deviation and comparisons across groups were made using one-way analysis of variance. Tukey's post hoc test was applied, with statistical significance set at $P < 0.05$.

RESULTS

Bruceine A alleviates histopathological lung injury and reduces alveolar apoptosis in ARDS mice triggered by LPS

To evaluate the protective role of BA against LPS-induced lung injury, histopathological changes, lung injury scoring, pulmonary edema (W/D ratio) and alveolar epithelial apoptosis were examined. As shown via H&E staining (Fig. 2A), the Sepsis group displayed severe lung damage, including alveolar wall thickening, capillary congestion, and inflammatory infiltration. In contrast, BA administration markedly reduced these lesions. Lung injury scores decreased from 3.85 ± 0.29 in the Sepsis group to 1.23 ± 0.31 in the BA group and 1.17 ± 0.27 in the Dex group ($P < 0.01$) (Fig. 2B). Similarly, the lung W/D ratios (Fig. 2C) were significantly reduced by BA (5.02 ± 0.35) and Dex (4.87 ± 0.41) treatments compared to the Sepsis (7.26 ± 0.44) group ($P < 0.01$). Moreover, TUNEL staining indicated that both BA (26.7% ± 1.7) and Dex (25.9% ± 1.0) significantly attenuated alveolar epithelial cell apoptosis induced by LPS (37.5% ± 1.8) ($P < 0.01$). Importantly, there was no significant difference

between the BA and Dex groups, indicating comparable efficacy (Fig. 2D-E). These data confirmed that BA had comparable efficacy to Dex in ameliorating LPS-induced lung injury.

Bruceine A modulates inflammatory cytokine profiles in LPS-induced ARDS

Next, the cytokine levels were characterized to evaluate the anti-inflammatory impact of BA versus Dex. In both serum and BALF, LPS exposure notably enhanced TNF-α, IL-6, as well as IL-1β, while markedly decreased IL-10 ($P < 0.01$) (Fig. 3). BA administration effectively suppressed TNF-α, IL-6 and IL-1β elevation, while restoring IL-10 levels significantly relative to the Sepsis group ($P < 0.01$). These cytokine modulation effects of BA were comparable to those of Dex, indicating that BA exerted a potent anti-inflammatory effect similar to conventional glucocorticoid therapy.

Bruceine A shifts macrophage polarization from pro-inflammatory M1 to anti-inflammatory M2 phenotype in LPS-driven ARDS

To gain deeper mechanistic insight, we assessed macrophage polarization. Both BA and Dex significantly suppressed M1 indicators (iNOS, COX-2) and promoted M2 indicators (Arg-1, YM1) ($P < 0.01$), indicating a shift towards anti-inflammatory macrophage phenotype (Fig. 4A-B). Immunohistochemical results further confirmed the shift in macrophage phenotype (Fig. 4C-D). Quantification of immunohistochemistry results showed that the percentage of iNOS-positive staining area was significantly reduced in BA-treated mice (0.05 ± 0.001) compared to the Sepsis group (0.07 ± 0.001) ($P < 0.01$), whereas the percentage of CD206-positive staining area was significantly increased (BA: 0.06 ± 0.002 vs. Sepsis: 0.05 ± 0.002, $P < 0.05$). Although the absolute values appear numerically close, these data represent normalized percentages of positive staining area and the statistical differences reflect reproducible biological effects. Notably, BA demonstrated similar effects as Dex, confirming its potent immunomodulatory capabilities.

Bruceine A inhibits NF-κB signaling activation in LPS-driven ARDS

Given the central importance of NF-κB signaling during inflammatory responses, its activity was assessed by Western blot detection of p-p65 and IκBα. LPS markedly increased p-NF-κB p65 levels while decreasing IκBα expression ($P < 0.01$), indicative of NF-κB activation. Treatment with BA significantly reversed these alterations, similarly to Dex ($P < 0.01$), suggesting effective suppression of NF-κB activation (Fig. 5). This inhibitory impact of BA on NF-κB signaling might underlie its anti-inflammatory action in ARDS.

DISCUSSION

BA possesses diverse pharmacological activities, including anti-inflammatory, anticancer and immunomodulatory effects and has been investigated in multiple disease models (Wang, *et al*., 2024a). However, its function and underlying immunomodulatory mechanisms in sepsis-associated ARDS remain poorly understood. Our findings show that BA protects against LPS-induced ARDS in mice by reducing lung damage, modulating cytokines, promoting M2 polarization and suppressing NF-κB signaling. BA markedly improved lung histopathology, as demonstrated by decreased alveolar collapse, reduced inflammatory infiltration and pulmonary edema. Moreover, TUNEL assay confirmed a reduction in alveolar epithelial cell apoptosis (from $37.5\% \pm 1.8$ to $26.7\% \pm 1.7$). These protective effects were comparable to Dex, with no statistically significant difference between BA and Dex in these parameters.

A hallmark of ARDS is cytokine storm, primarily driven by excessive secretion of TNF-α, IL-6 and IL-1β, coupled with insufficient IL-10 levels (Liu, *et al*., 2022b, Zhou, *et al*., 2025). ELISA analysis demonstrated that BA notably reduced TNF-α, IL-6 and IL-1β levels, while markedly elevating IL-10 expression in both serum and BALF. These results align with earlier research on resveratrol, a plant-derived compound known to attenuate ARDS via cytokine regulation (Tang, *et al*., 2022). While structurally distinct, both BA and resveratrol target key inflammatory mediators, suggesting that natural compounds may offer multi-targeted therapeutic strategies in ARDS.

Macrophages are central regulators in ARDS pathogenesis. Under inflammatory stress, M1 macrophages dominate and secrete damaging cytokines, whereas M2 macrophages support resolution and repair (Wang and Wang, 2023, Arora, *et al*., 2018). In this study, LPS-induced ARDS mice caused upregulation of M1-related proteins (iNOS, COX-2) together with suppression of M2-related proteins (Arg-1, Ym1, CD206), indicating that M1 macrophages dominated under inflammatory conditions, thereby amplifying pro-inflammatory responses. By shifting macrophages from M1 to M2, BA restored immune balance, consistent with other studies highlighting macrophage polarization as a therapeutic target (Luo, *et al*., 2022). Notably, the extent of BA-induced M2 polarization was statistically comparable to that of Dex, indicating that BA exerts potent immunomodulatory effects equivalent to established anti-inflammatory agents.

The NF-κB pathway is pivotal in mediating inflammatory gene transcription in ARDS (Zheng, *et al*., 2024). In this study, BA significantly downregulated p-NF-κB p65 and restored IκBα expression, suppressing this pro-inflammatory pathway. This finding is consistent with prior findings showing that NF-κB inhibition alleviates ARDS, such as in the study by Zhuang *et al*., using statins (Zhuang, *et al*., 2023). Moreover, our data suggest that BA's dual effect, both on cytokines and macrophage phenotype, may be at least partially mediated through NF-κB suppression.

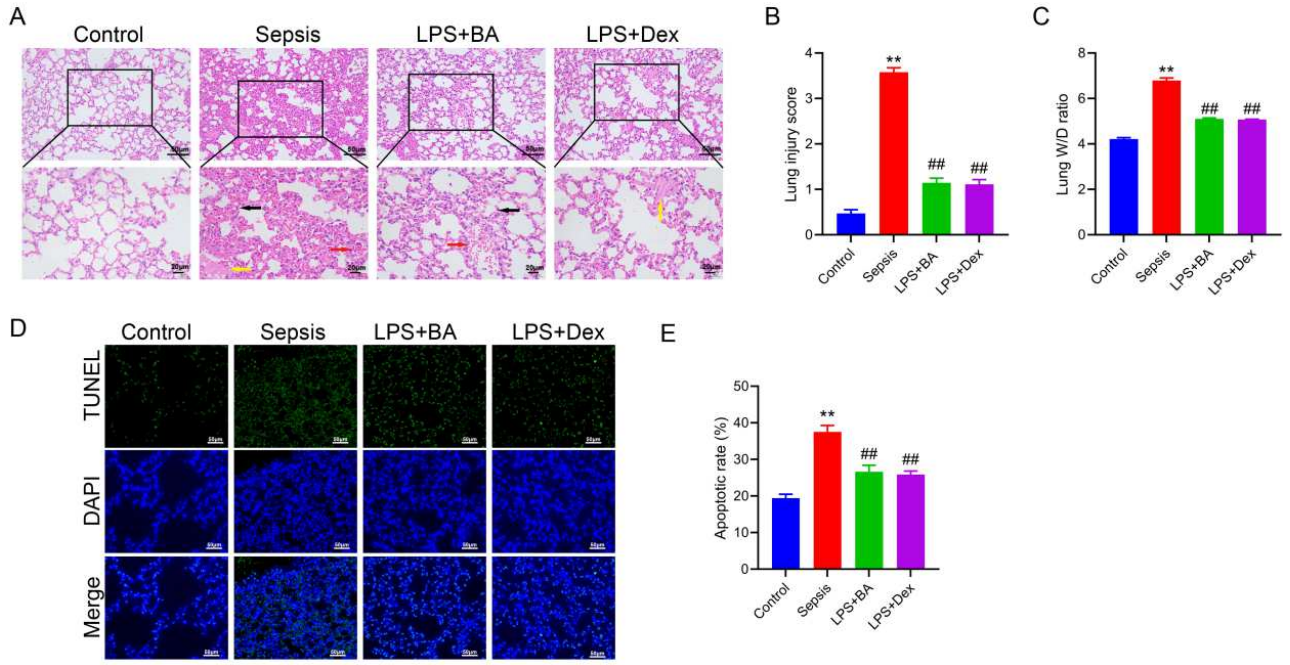

Fig. 2: Bruceine A attenuates lung injury and alveolar apoptosis induced by LPS.
(A) Representative H&E-stained lung tissue sections from Control, Sepsis, LPS+BA, and LPS+Dex groups. Arrows indicate inflammatory cell infiltration (Black arrows indicate alveolar wall thickening, red arrows indicate inflammatory infiltration, and yellow arrows indicate alveolar collapse). (B) Quantification of lung injury score. (C) Lung wet/dry (W/D) weight ratio. (D) Representative fluorescence images showing TUNEL-positive apoptotic cells (green), DAPI-stained nuclei (blue), and merged images. (E) Quantification of alveolar epithelial apoptosis. Statistical analysis was performed using one-way ANOVA followed by Tukey's post hoc test. Data are expressed as mean ± SD (n = 9). **P < 0.01 vs. Control; ##P < 0.01 vs. Sepsis. No significant difference was observed between BA and Dex groups.

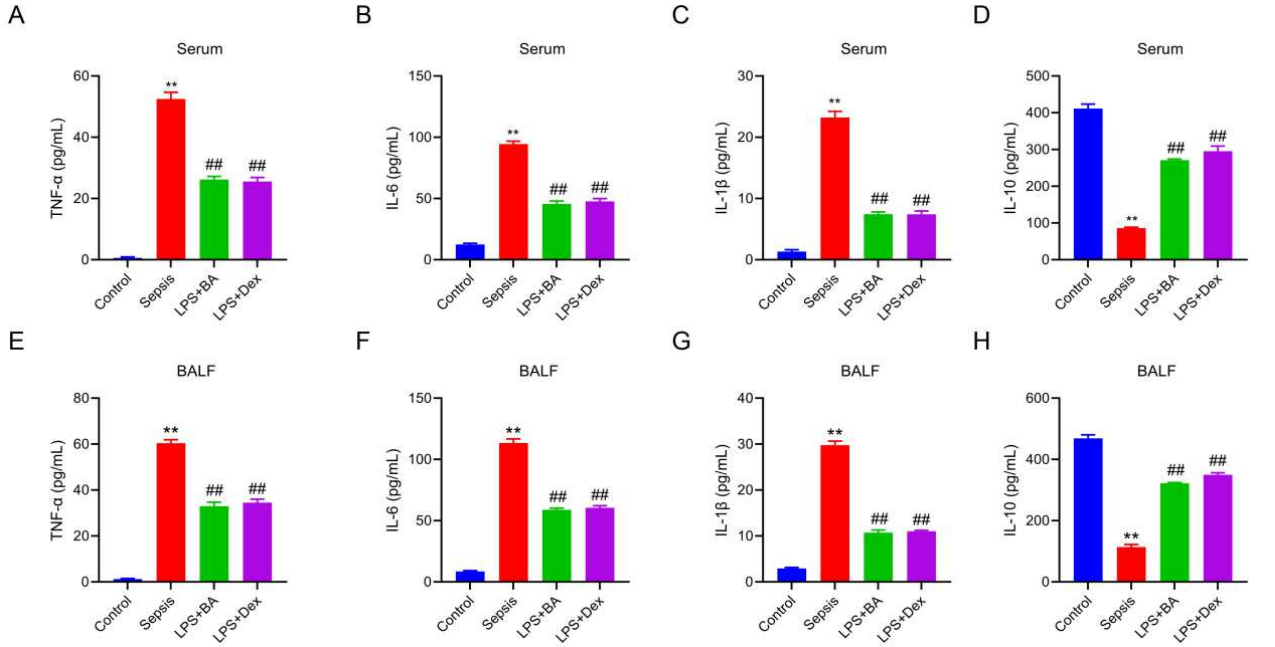

Fig. 3: Bruceine A regulates inflammatory cytokines in serum and BALF.
(A–D) Serum levels of TNF-α (A), IL-6 (B), IL-1β (C), and IL-10 (D). (E–H) Corresponding cytokine levels in bronchoalveolar lavage fluid (BALF). Statistical analysis was performed using one-way ANOVA followed by Tukey's post hoc test. Data are presented as mean ± SD (n = 9). **P < 0.01 vs. Control; ##P < 0.01 vs. Sepsis.

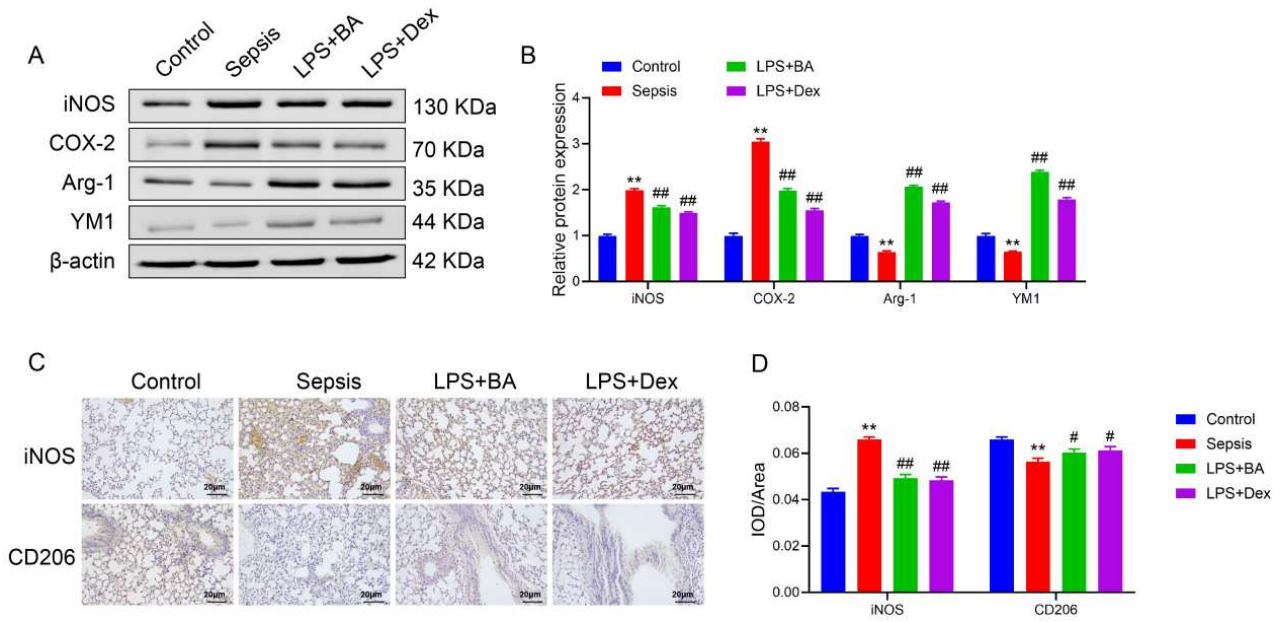

Fig. 4: Bruceine A modulates macrophage polarization in lung tissues.
(A-B) Western blot analysis of macrophage markers: iNOS, COX-2 (M1), Arg-1, YM1 (M2). (C-D) Immunohistochemistry staining for iNOS and CD206. Quantification is presented as percentage of positive staining area (% positive area). Statistical analysis was performed using one-way ANOVA followed by Tukey's post hoc test. Data represent mean ± SD (n = 9). *P < 0.05, **P < 0.01 vs. Control; #P < 0.05, ##P < 0.01 vs. Sepsis.

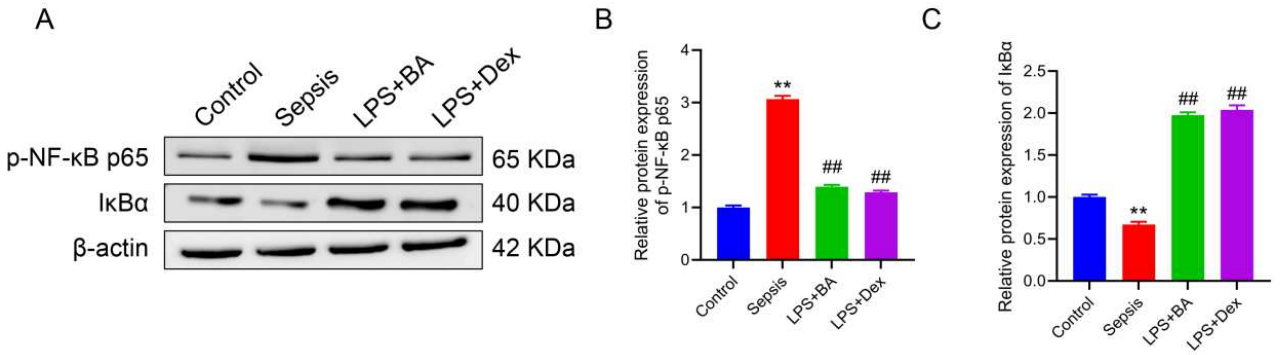

Fig. 5: Bruceine A suppresses NF-κB signaling activation in lung tissues.
(A) Representative Western blot images showing expression of phosphorylated NF-κB p65 (p-NF-κB p65) and IκBα proteins. (B) Quantification of p-NF-κB p65 relative expression. (C) Quantification of IκBα relative expression. Statistical analysis was performed using one-way ANOVA followed by Tukey's post hoc test. Data represent mean ± SD (n = 9). **P < 0.01 vs. Control; ##P < 0.01 vs. Sepsis.

However, we acknowledge that these results demonstrate a correlation. More definitive mechanistic validation, such as co-treatment with NF-κB inhibitors or use of knockout models, is warranted.

Despite its promising therapeutic effects, this study has several limitations. The use of a single LPS-induced ARDS model reflects only the acute inflammatory phase and may not capture the full complexity of clinical ARDS. A single BA dose and treatment duration were applied, without dose-response or time-course evaluation. Future work will include dose–response and time-course studies and formal pharmacokinetic profiling (bioavailability, half-life, tissue distribution) to link exposure with effect in ARDS. Lung function parameters such as gas exchange or oxygenation index were not assessed. Thus, the findings rely solely on molecular, histological and biochemical endpoints rather than functional validation. Mechanistically, the observed modulation of macrophage polarization and NF-κB signaling remains correlative and other pathways (e.g., JAK-STAT, PI3K/Akt, Nrf2) were not examined. Moreover, the study focused on macrophages, while neutrophils, T cells, Th1/Th17 responses and alveolar epithelial cells-key contributors to ARDS-were not investigated. Finally, the long-term safety, pharmacokinetics and metabolic stability of BA remain unknown. Future studies should address these gaps through expanded models, functional assessments and pharmacokinetic analyses.

Collectively, these findings indicate that BA exerts protective effects against inflammatory lung injury primarily by modulating macrophage polarization and NF-κB signaling. Nevertheless, further mechanistic and translational studies are required to confirm these results.

CONCLUSION

In conclusion, BA attenuates lipopolysaccharide-induced ARDS in mice through immunomodulatory effects on cytokine production, macrophage polarization and NF-κB pathway inhibition.

Acknowledgement
Not applicable.

Authors' contributions
Jianlei Lv and Kang Huang conceived and designed the study. Songbai Wu and Min Liu performed the animal experiments and data acquisition. Kang Huang supervised the entire project and revised the manuscript. All authors contributed to data interpretation, manuscript writing and approved the final version of the manuscript.

Funding
There was no funding.

Data availability statement
The datasets generated during and/or analysed during the current study are available from the corresponding author on reasonable request.

Ethical approval
All procedures involving animals were carried out in accordance with ethical standards and approved by the Animal Ethics Committee of The First Hospital of Changsha (Approval No. ethic-15-354-cs).

Conflict of interest
The authors declare that they have no competing interests.

REFERENCES

Arina Pietro and Mervyn Singer (2021). Pathophysiology of sepsis. *Curr. Opin. Anesthesio.,* **34**: 77-84.

Arora S, K Dev, B Agarwal, P Das and MA Syed (2018). Macrophages: Their role, activation and polarization in pulmonary diseases. *Immunobiology,* **223**: 383-396.

Banavasi Harsha, Paul Nguyen, Heba Osman and Ayman O Soubani (2021). Management of ARDS–What works and what does not. *Am J Med Sci.,* **362**: 13-23.

Chang Xinyan, Shaojun Li, Yueqiang Fu, Hongxing Dang and Chengjun Liu (2022). Safety and efficacy of corticosteroids in ARDS patients: A systematic review and meta-analysis of RCT data. *Resp. Res.,* **23**: 301.

Chastain Daniel B, Megan Spradlin, Hiba Ahmad and Andrés F Henao-Martínez (2024). Unintended consequences: Risk of opportunistic infections associated with long-term glucocorticoid therapies in adults. *Clin Infect Dis.,* **78**: e37-e56.

Cheng Peiyong, Shuangyan Li and Huaiyong Chen (2021). Macrophages in lung injury, repair and fibrosis. *Cells* **10**: 436.

Feng Jun, Lina Liu, Yang He, Min Wang, Daixing Zhou and Junshuai Wang (2021). Novel insights into the pathogenesis of virus-induced ARDS: Review on the central role of the epithelial-endothelial barrier. *Expert Rev. Clin. Immu.,* **17**: 991-1001.

Ge J, H Yang, N Yu, S Lin and Y Zeng (2024). Wogonin alleviates sepsis-induced acute lung injury by modulating macrophage polarization through the SIRT1-FOXO1 pathways. *Tissue Cell,* **88**: 102400.

Gorman Ellen A, Cecilia M O'Kane and Daniel F McAuley (2022). Acute respiratory distress syndrome in adults: Diagnosis, outcomes, long-term sequelae, and management. *The Lancet.,* **400**: 1157-1170.

Gouda NA, SO Alshammari, MAS Abourehab, QA Alshammari and A Elkamhawy (2023). Therapeutic potential of natural products in inflammation: Underlying molecular mechanisms, clinical outcomes, technological advances and future perspectives. *Inflammopharmacology,* **31**: 2857-2883.

He Xiao, Jiahui Wu, Ting Tan, Wenjing Guo, Ziwei Xiong, Shilin Yang, Yulin Feng and Quan Wen (2021). Quassinoids from Brucea javanica and attenuates lipopolysaccharide-induced acute lung injury by inhibiting PI3K/Akt/NF-κB pathways. *Fitoterapia.,* **153**: 104980.

Huang Qianrui, Yue Le, Shusheng Li and Yi Bian (2024). Signaling pathways and potential therapeutic targets in acute respiratory distress syndrome (ARDS). *Resp. Res.,* **25**: 30.

Kang HJ, J Mao, MJ Kim, KW Yoon, GD Eom, KB Chu, EK Moon and FS Quan (2023). The detection of Toxoplasma gondii ME49 infections in BALB/c mice using various techniques. *Parasites Hosts Dis.,* **61**: 418-427.

Ke H, X Wang, Z Zhou, W Ai, Z Wu and Y Zhang (2021). Effect of weimaining on apoptosis and Caspase-3 expression in a breast cancer mouse model. *J Ethnopharmacol.,* **264**: 113363.

Kim SM, JH Min, JH Kim, J Choi, JM Park, J Lee, SH Goo, JH Oh, SH Kim, W Chun, KS Ahn, S Kang and JW Lee (2022). Methyl p-hydroxycinnamate exerts anti-inflammatory effects in mouse models of lipopolysaccharide-induced ARDS. *Mol. Med. Rep.,* **25**(1): 37.

Liu Chang, Kun Xiao and Lixin Xie (2022). Advances in the regulation of macrophage polarization by mesenchymal stem cells and implications for ALI/ARDS treatment. *Front Immunol* **13**: 928134.

Liu D, Y Zhang, B Bai, X Xiong, Q Zhou and R Shi (2025). Integration of single-cell RNA sequencing and network pharmacology to elucidate the effect of Yantiao Formula

on alleviating ALI by regulating the polarization of alveolar macrophages. *J Ethnopharmacol.,* **343**: 119436.

Liu Shuyu, Zhenhan Deng, Kang Chen, Shengsheng Jian, Feifei Zhou, Yuan Yang, Zicai Fu, Huanyu Xie, Jianyi Xiong and Weimin Zhu (2022). Cartilage tissue engineering: From proinflammatory and anti-inflammatory cytokines to osteoarthritis treatments. *Mol. Med. Rep.,* **25**: 99.

Luan G, F Pan, L Bu, K Wu, A Wang and X Xu (2021). Butorphanol Promotes Macrophage Phenotypic Transition to Inhibit Inflammatory Lung Injury via κ Receptors. *Front Immunol.,* **12**: 692286.

Luo Jing, Jin Wang, Jing Zhang, Aming Sang, Xujun Ye, Zhenshun Cheng and Xinyi Li (2022). Nrf2 deficiency exacerbated CLP-induced pulmonary injury and inflammation through autophagy-and NF-κB/PPARγ-mediated macrophage polarization. *Cells* **11**: 3927.

Nie Y, B Yang, J Hu, L Zhang and Z Ma (2021). Bruceine D ameliorates the balance of Th1/Th2 in a mouse model of ovalbumin-induced allergic asthma via inhibiting the NOTCH pathway. *Allergol Immunopath.,* **49**: 73-79.

Pérez Salvador and Sergio Rius-Pérez (2022). Macrophage polarization and reprogramming in acute inflammation: A redox perspective. *Antioxidants,* **11**: 1394.

Sygitowicz Grażyna and Dariusz Sitkiewicz (2021). Molecular mechanisms of organ damage in sepsis: An overview. *Braz J. Infect Dis.,* **24**: 552-560.

Tang Y, W Fu, K Wei, L Liu, S Wu and W Tang (2022). The therapeutic efficacy of resveratrol for acute lung injury-A meta-analysis of preclinical trials. *Front Pharmacol.,* **13**: 963245.

Wang Ke, Jinlu Shang, Chao Tao, Mingquan Huang, Daiqing Wei, Liuxuan Yang, Jing Yang, Qingze Fan, Qian Ding and Meiling Zhou (2024). Advancements in betulinic acid-loaded nanoformulations for enhanced anti-tumor therapy. *Int. J. Nanomed*., pp.14075-14103.

Wang L, J Wang, L Han and T Chen (2024). Palmatine attenuated lipopolysaccharide-induced acute lung injury by inhibiting m1 phenotype macrophage polarization via NAMPT/TLR2/CCR1 Signaling. *J Agric Food Chem*.

Wang Lin and Chengqi He (2022). Nrf2-mediated anti-inflammatory polarization of macrophages as therapeutic targets for osteoarthritis. *Front Immunol.,* **13**: 967193.

Wang Ziyi and Zhong Wang (2023). The role of macrophages polarization in sepsis-induced acute lung injury. *Front Immunol.,* **14**: 1209438.

Zeng T, Y Zhou, Y Yu, JW Wang, Y Wu, X Wang, L Zhu, LM Zhou and LH Wan (2023). rmMANF prevents sepsis-associated lung injury via inhibiting endoplasmic reticulum stress-induced ferroptosis in mice. *Int. Immunopharmacol.,* **114**: 109608.

Zhang Chaozheng, Yuening Cao, Yi Zuo, Hongbin Cheng, Changqun Liu, Xila Xia, Bo Ren, Yun Deng, Maolin Wang and Jun Lu (2023). Bruceine a exerts antitumor effect against colon cancer by accumulating ROS and suppressing PI3K/Akt pathway. *Front Pharmacol.,* **14**: 1149478.

Zhang J, C Wang, H Wang, X Li, J Xu and K Yu (2021). Loganin alleviates sepsis-induced acute lung injury by regulating macrophage polarization and inhibiting NLRP3 inflammasome activation. *Int Immunopharmacol.,* **95**: 107529.

Zheng Jiajing, Ying Li, Xianbin Kong and Jinhe Guo (2024). Exploring immune-related pathogenesis in lung injury: Providing new insights Into ALI/ARDS. *Biomed Pharmacother.,* **175**: 116773.

Zhou K, Q Qin and J Lu (2025). Pathophysiological mechanisms of ARDS: A narrative review from molecular to organ-level perspectives. *Respir. Res.,* **26**: 54.

Zhuang Xiaoli, Yu Jiang, Xiaofang Yang, Lin Fu, Lan Luo, Ziyuan Dong, Ju Zhao and Feilong Hei (2023). Advances of mesenchymal stem cells and their derived extracellular vesicles as a promising therapy for acute respiratory distress syndrome: From bench to clinic. *Front Immunol.,* **14**: 1244930.